Tensile and Deformation Behavior of Auxetic Plied Yarns

Wing Sum Ng, Hong Hu*

Institute of Textiles and Clothing, The Hong Kong Polytechnic University, Hung Hom, Kowloon, Hong Kong
*Corresponding author: hu.hong@polyu.edu.hk

Abstract

This paper presents an experimental study of tensile and deformation behavior of an auxetic plied yarn structure. The basic configuration of the plied structure formed with two soft yarns and two stiff yarns was firstly introduced. Based on this 4-ply helix structure, six kinds of yarn samples were made by different combinations of soft yarns, stiff yarns and twist levels. These yarn samples were first tested and the effects of different design parameters were analyzed. Apart from the tensile test, changes in the internal structure of two samples upon stretching were also studied through microscopic examination. Finally, double helix yarn and 6-ply auxetic yarn were made for a comparative purpose to investigate the effect of helical structure. The study shows that all of the 4-ply auxetic yarn samples exhibit negative Poisson's ratio (NPR) throughout the entire tensile process, and the magnitude of NPR gets larger with a smaller soft yarn diameter, a higher tensile modulus of stiff yarn and a lower twist level. The study also shows that auxetic behavior inside the 4-ply structure is generated by the interplay between the soft yarns and stiff yarns and 4-ply auxetic yarns have the advantages to produce immediate auxetic effect upon stretching.

Keywords: Auxetic yarn; negative Poisson's ratio; deformation behavior; auxetic textiles

1. Introduction

Materials with a negative Poisson's ratio are known as auxetics. They laterally expand when stretched or contract when compressed [1]. Real interest in auxetic materials began when Lakes developed the first negative Poisson's ratio material in 1987, which was a polyurethane foam with re-entrant structure made by triaxial compression and heat treatment [2]. Ever since, a variety of man-made auxetic materials have been manufactured and synthesized, including but not limited to microporous polymers[3], honeycomb structures [4], polymeric and metallic foams [5], auxetic composites [6] and molecular auxetic materials [7]. Fabrication of auxetic materials has long captivated the attention of researchers because auxeticity in materials may enhance certain mechanical properties over their non-auxetic counterparts, including fracture toughness, shear stiffness, indentation resistance, pullout resistance, synclastic curvature, sound absorption capacity and variable permeability [8-10].

In the textile and clothing sector, a wide range of auxetic textiles have been made and shown great potential application in many areas. In general, there are two approaches to fabricate auxetic textiles. The first approach is to use conventional fibers and yarns to create auxetic effect by knitting or weaving them in a special geometrical configuration [11, 12]. A variety of weft-knitted and warp-knitted auxetic fabrics have been produced with this method in the recent years [13-16]. However, their application has been rather limited by the three dimensional structure. The second approach is to use auxetic fibers [17-18] and yarns [19-20] to fabricate auxetic textiles directly, such that auxetic effect can be created by simple weaving or knitting patterns. Creating

auxetic effect at the yarn stage is a new and interesting area of research, because unlike auxetic fibers which are often manufactured under complicated processing conditions, helical auxetic yarn (HAY) can be made simply by winding or twisting different conventional filaments together with existing spinning machinery and standard manufacturing techniques [21].

Double helix yarn (DHY) is the first reported HAY in the field of auxetic textiles. It was proposed by Hook in 2003 [22], and is formed by winding a stiff yarn around a soft core yarn to produce the auxetic effect. The basic structure and mechanics of the DHY have been widely studied. Wright, Sloan and Evans carried out a finite element analysis and an experimental study to investigate the influence of structural and material parameters on the auxetic performance of the DHY [21, 23]. Du et al. conducted a theoretical analysis to predict the auxetic performance of the DHY for any given tensile strain and an experimental study afterward to verify the accuracy of the model [24, 25]. Sibal and Rawal also proposed a DHY system to predict the auxetic behavior of the DHY through energy minimization approach [26]. Bhattacharya et al. investigated the core-indentation effects on the auxetic behavior of the DHY [27].

Apart from the investigations on structure and mechanics of the DHYs, previous research works also focused on making woven fabrics and composites with different arrangement of DHYs [28, 29]. Anyhow, DHYs were allocated in one direction only such that anisotropic properties are exhibited. Auxetic textiles made of HAYs display wide porosity variation under tensile load, which is an attractive feature for certain applications, such as smart bandage which can control drug delivery for wound healing,

filter which can filter out particles of different sizes under different extension levels and blast-proof curtain which can catch the debris coming up from bomb explosion [30-32].

Studies of HAY were predominantly focused on DHY, until recently, Ge et al. has developed a new approach to produce negative Poisson's ratio in yarn with a specific 4-ply structure [33]. The work of Ge et al. included a geometric analysis to calculate the Poisson's ratio values of the auxetic plied yarn for any given tensile strain, and the experimental result revealed that the geometrical model was only capable of predicting the Poisson's ratio at high strains.

It should be pointed out that development and investigation on this kind of auxetic plied yarn are still in its early stages. Although Ge et al. have proven that stretching the auxetic plied yarn can result in a net increase in the effective diameter of the yarn, factors that influence its tensile properties and auxetic behavior are not well understood and characterized. Moreover, capturing consecutive images during tensile testing is a two-dimensional assessment which is only capable to measure the growth of yarn along the plane of elongation, but not able to provide an in-depth understanding to the changes of each constituent yarn under axial tension load.

Therefore, the aim of this paper is to experimentally study the mechanical and deformation properties of this kind of 4-ply auxetic yarn under tensile load. Six kinds of samples were manufactured with two types of stiff yarns, two types of soft yarns and three different twist levels. These yarns were tested and characterized in terms of their

tensile properties and auxetic behavior. The effects of different parameters of the yarn under axial extension were analyzed, including diameter of soft yarn, tensile modulus of stiff yarn and twist level. On the other hand, cross-sectional images of two samples at various strain levels were acquired and processed to examine the cross-sectional deformation mechanism of the yarns, and to analyze their differences brought by two different stiff yarns. In addition, double helix yarn and 6-ply auxetic yarn were made for a comparative purpose to evaluate the effect on the auxetic behavior arising from different helical structures.

2. Different helical structures and their respective deformation mechanism

Two basic types of HAYs can be defined according to the deformation mechanism that give rise to NPR, i.e. the double helix yarn and the auxetic plied yarn. As schematically shown in Figure 1a, DHY consists of two filaments in which a high stiffness filament is twisted in a helical manner around a straight core filament with a larger diameter and lower stiffness [21]. When DHY is being stretched longitudinally, two filaments gradually interchange their positions. As shown in Figure 1b, the high stiffness filament tends to straighten, thereby causing the low stiffness core filament to helically wrap around it and resulting in a net increase in the effective diameter of the yarn.

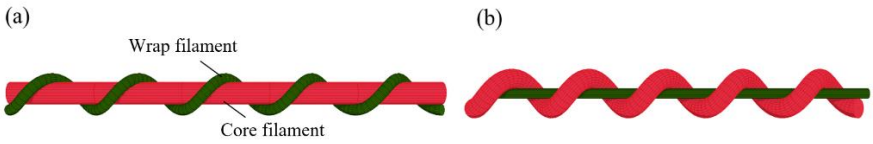

Figure 1 DHY: (a) at rest; (b) under tension.

Another new type of HAY, the auxetic plied yarn, is schematically shown in Figure 2a. It can be seen that two soft yarns of a relatively large diameter are arranged in the center position while two stiff yarns are spiraling around them to form a 4-ply helix structure [34]. Compared with the DHY which has a filament helically wrapping around a barely twisted filament and being unbalanced, the auxetic plied yarn is more stable so that twist regularity of the auxetic yarn can be improved.

Deformation mechanism of the auxetic plied yarn is different from that of DHY in which the auxetic behavior is caused by the migration of stiff yarns in the plied structure. As shown in Figures 2b and 2c, when the auxetic yarn is stretched along its longitudinal axis, the stiff yarns will tend to migrate to the center and push the soft yarns outward, resulting in a lateral expansion of the auxetic yarn's maximal width. It should be further noted that this kind of auxetic plied yarn includes, but not limited to a 4-ply structure. For instance, as shown in Figure 3a, auxetic plied yarn can be produced in a 6-ply structure by arranging three soft yarns and three stiff yarns alternatively to create auxetic effect with the same mechanism as shown in Figure 3b. In this study, we remained focus here on the auxetic plied yarn in 4-ply structure. For comparative purposes, one kind of soft yarn and one kind of stiff yarn were selected to fabricate DHY and 6-ply auxetic yarn, and compare with the 4-ply auxetic yarn to investigate the effect on the auxetic behavior arising from different helical structures.

Figure 2 4-ply auxetic yarn: (a) at rest; (b) under tension; (c) at different states in cross-section view.

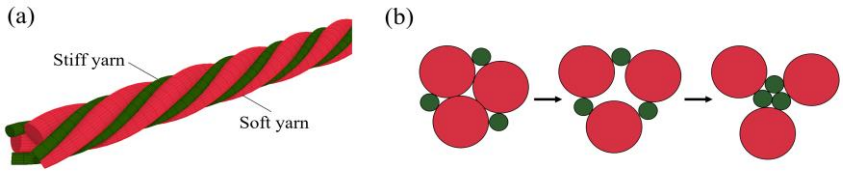

Figure 3 6-ply auxetic yarn: (a) side view; (b) cross-section view at different states.

3. Experimental details

3.1 Fabrication of auxetic yarn samples

To quantitatively evaluate the effect of different parameters on the mechanical properties of the 4-ply auxetic yarn, four kinds of single yarns were procured for fabricating the yarn samples and their specifications are shown in Table 1. Firstly, to make clear the effect of diameter ratio, two different polyester covered rubber cords were used as soft yarns, with a diameter of 2.18 mm and 1.14 mm, respectively. Secondly, to investigate the effect of tensile modulus of stiff yarn, polyester covered monofilament cord and waxed polyester cord were used as stiff yarns, with an elastic modulus of 630 MPa and 1307 MPa respectively. As shown in Figure 4, a helical auxetic yarn spinner was built to fabricate lab-scale lengths of yarn samples for examination. With the aid of this prototype, auxetic yarns with different helical

structures can be made by feeding different amount of single yarn to the spinning device. To produce a 4-ply auxetic yarn, two strands of soft yarns and two strands of stiff yarns are alternately arranged and fed through the yarn guiding board which is fixed at one end of the spinning device. Ends of the constituent yarns are wrapped with adhesive tape in which the stiff yarns are separated by the soft yarns while the soft yarns are adhered to one another. The wrapped yarns are then held in the clamp which is fixed on a movable board connected with a rotating handle. In making ply yarns from spun strands, the handle is manually rotated and moved backward simultaneously to draw free ends of constituent yarns to the yarn forming zone, such that the constituent yarns are combined into 4-ply helix yarn after it passed through the yarn guiding board. The amount of twist inserted is determined by the length of the yarn fed through the yarn guiding board and by the number of twists imparted over that length. Therefore, the twist can be modified by keeping either parameter constant and varying the other. To increase the twist level, rotational speed can be kept constant while decreasing the yarn drawing speed; or the yarn drawing speed can be kept constant while increasing the rotational speed. The same result will be obtained in either case.

Details of the yarn samples are listed in Table 2. Different soft yarns and stiff yarns were combined together to fabricate 4-ply auxetic yarn samples with a twist of 51 turns/m. Additional twist levels of 35 turns/m and 65 turns/m were employed for sample A-1 to evaluate the effect of twist level, such that a total of six different 4-ply auxetic yarn samples were produced. Furthermore, yarn A and yarn 1 were chosen to fabricate additional DHY and 6-ply auxetic yarn samples (named A-1-D and A-1-T)

with a twist of 51 turns/m to investigate the effect of helical structures on the auxetic behavior of the HAY.

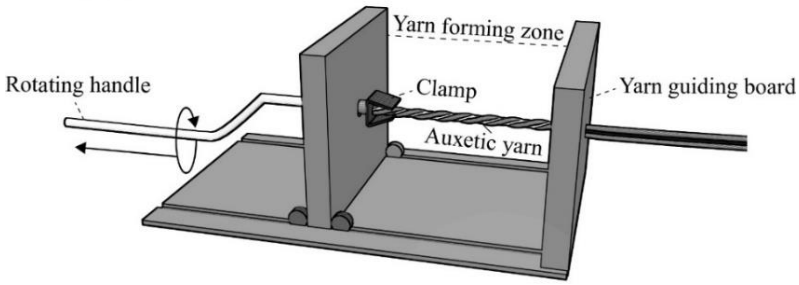

Figure 4 Schematic diagram of the helical auxetic yarn spinning device.

Table 1 Specifications of the single yarns.

Single Yarn Code	Material	Diameter (mm)	Elastic modulus (MPa)	Elongation at break (%)
A	Polyester covered rubber cord	2.18	13	189
B	Polyester covered rubber cord	1.14	8	222
1	Polyester covered monofilament cord	0.87	630	20
2	Waxed polyester cord	0.77	1307	10

Table 2 Construction characteristics of the HAYs.

Sample Code	Yarn type	Yarn twist (turns/m)	Yarn composition		Side view
			Soft yarn	Stiff yarn	
A-1	4-ply	51	A	1	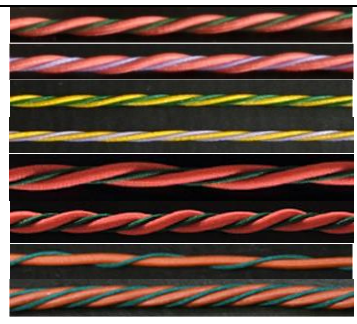
A-2	4-ply	51	A	2	
B-1	4-ply	51	B	1	
B-2	4-ply	51	B	2	
A-1-L	4-ply	35	A	1	
A-1-H	4-ply	65	A	1	
A-1-D	Double helix	51	A	1	
A-1-T	6-ply	51	A	1	

3.2 Tensile testing

The above eight kinds of HAY samples were subjected to tensile test to evaluate their tensile properties and auxetic behavior under different extension levels, and the specifications of the experimental design are listed in Table 3. Comparisons were made on different groups of yarn samples to study the effect of each design parameter on the mechanical properties of the 4-ply auxetic yarn, and the effect of helical structures on the auxetic behavior of the HAYs.

Set-up of the testing system is shown in Figure 5. Tensile measurements were conducted on INSTRON 4411 mechanical testing machine at a gauge length of 250mm and a crosshead speed of 50mm/min until breakage. Specimens were tested with a pre-tension of 0.5N. One side of yarn end is secured in the upper clamp, and the other side is applied with pre-tension before closing the lower clamp to ensure that all the slack or kinks from the specimens were removed without appreciable stretching. Three tests were conducted for each type of sample to obtain the average tensile properties. To make comparison between different yarns possible, the load and elongation data gathered during the test were converted to tensile stress and strain, where the stress was calculated based on the initial cross-sectional area of the yarn measured in the cross-sectional image.

In order to measure the auxetic behavior of the HAY samples during different period of extension, a high-resolution CMOS camera was placed in front of the tensile testing machine to capture consecutive images of the tested sample at 2-second intervals

during the experiment, which corresponded to a 0.7% interval of the tensile strain ε_x. The raw images were saved in the computer and converted to greyscale, and then binary image. As shown in Figure 6, the binary images provided the maximal thickness of the yarn sample at the initial state D_0 without tension and that at the stretched state D. Once the values of D_0 and D were obtained by counting the number of pixels in the images, transverse strain ε_y could be calculated from equation (1).

$$\varepsilon_y = \frac{D - D_0}{D_0} \quad (1)$$

As the tensile strain ε_x was directly provided by the tensile testing machine, Poisson's ratio of the HAY ν could be calculated from equation (2).

$$\nu = -\frac{\varepsilon_y}{\varepsilon_x} \quad (2)$$

Table 3 Specifications of the experimental design.

Group	Comparison	Parameters	Factor
1 2	A-1, B-1 A-2, B-2	Soft yarn diameter: 2.18 mm, 1.14 mm	Diameter of soft yarn
3 4	A-1, A-2 B-1, B-2	Stiff yarn tensile modulus: 630 MPa, 1307 MPa	Tensile modulus of stiff yarn
5	A-1-L, A-1, A-1-H	Yarn twist: 35 turns/m, 51 turns/m, 65 turns/m	Twist level
6	A-1-D, A-1, A-1-T	Yarn type: double helix, 4-ply, 6-ply	Helical structure

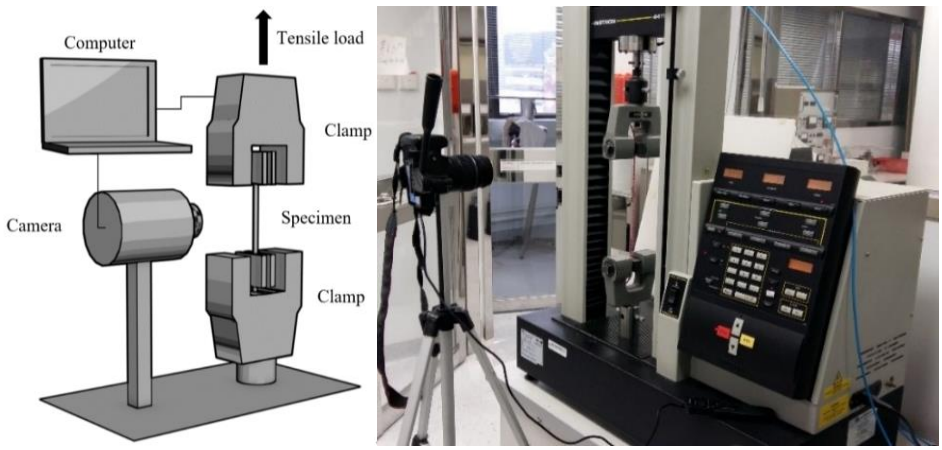

Figure 5 A schematic diagram and photograph of the tensile testing system.

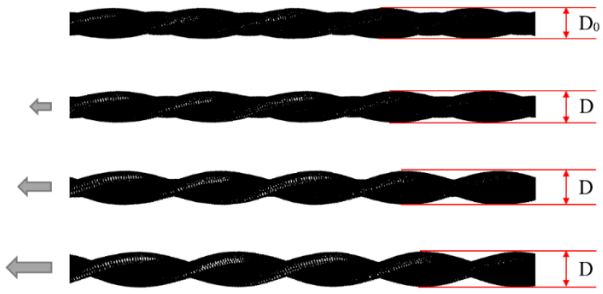

Figure 6 Binary images of the 4-ply auxetic yarn structure at initial state and stretched states.

3.3 Cross-sectional deformation analysis

In this study, samples A-1 and A-2 were selected to investigate the cross-sectional deformation behavior of 4-ply auxetic yarn and the differences brought by the two stiff yarns with vastly different tensile moduli. This pair of 4-ply auxetic yarns was chosen because of their good optical properties, i.e. large diameter 4-ply auxetic yarns can be observed easily, such that clear edge can be obtained and this could facilitate later analysis. As shown in Figure 7, a device was made to prepare the cross-sectional samples, in which a plastic cylinder round bottle was used as a mold and a hole was drilled through the center of the bottle to pass the yarn through. A 20 cm length of yarn sample was inserted and secured by screws without extension. The starting position of the instrument was adjusted to a distance of 105mm, from nip to nip of the cross dowels along the yarn axis. After the yarn was introduced, the bottom of the bottle was sealed to avoid resin-leaking. Following this, extension could be applied. Except the first cross-sectional sample which should be produced under zero strain, extension was applied in an increment of 2mm each by moving the cogs upward and retightened the wing nuts. For sample A-1, axial extension was applied in 8 increments until a final

extension of 16mm, which corresponded to a strain from 0.00 to 0.15. For yarn A-2, since higher load was required to stretch the yarn, the plastic bottle crushed easily at high strain due to overtightening. Therefore, axial extension was applied in 6 increments until a final extension of 12mm only, which corresponded to a strain from 0.00 to 0.11. In order to freeze the auxetic yarn under specific strain, epoxy resin and hardener were mixed in a 10:1 ratio and poured into the bottle. To avoid interferences with transmission of light during microscopic examination, few drops of black ink were mixed in the solution as well. After several hours of consolidation under room temperature, the cross sectional sample was pulled out from the bottle and ground with sandpapers.

Three cross-sectional samples were prepared for each extension level, and these samples were viewed and captured under microscope with 20 times magnification. The cross-sectional images consist of 2048 x 1536 pixels and the length of one pixel is 3.289μm. Photoshop was used to convert the images to greyscale so that desired information could be represented in a condensed form for easy characterization. In addition, black and white adjustment was adopted to further improve the contrast of the images. From the cross-sectional images, variation in position and shape of the constituent yarns under different strains were observed. In addition, the images were processed to measure the cross-sectional parameters with the software Adobe Illustrator. As shown in Figure 8, the circumference of each constituent yarn was outlined and the maximal diameter of the 4-ply auxetic yarn (D_{max}) was measured. Poisson's ratios for the two samples were then calculated and compared with those obtained through tensile test measurements.

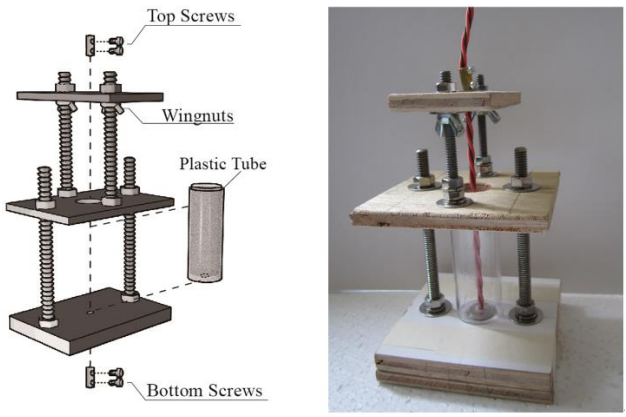

Figure 7 Schematic diagram and photograph of the cross-sectional sample preparation device.

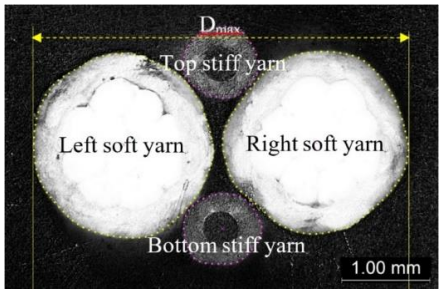

Figure 8 4-ply auxetic yarn measurements.

4. Results and discussion

4.1 Typical tensile and deformation behavior of the 4-ply auxetic yarn structure

Auxetic yarn sample A-2 is selected here as an example to discuss the typical tensile and deformation behavior of the 4-ply auxetic yarn structure. Its tensile stress-strain curve and those of its component single yarns are depicted in Figure 9a. In order to get a better view of those curves at low level of stress, an inset is also shown in Figure 9a. It can be seen that stiff yarn 2 has a much higher stiffness and a much lower degree of elongation than soft yarn A. Combining two strands of soft yarns and two strands of stiff yarns in a 4-ply helix structure, sample A-2 shows a higher elongation at break

than single stiff yarn, due to the obliquity effect in the 4-ply structure and variability in breaking extension brought by the soft yarns.

Figure 9a also shows that the typical tensile stress-strain curve of the 4-ply auxetic yarn structure can be divided into two stages. In the first stage, the auxetic yarn exhibits an initially low stiffness until it takes about 5 percent of the yarn's breaking strength. It is mainly governed by the tensile property of soft yarns, owning to the fact that high modulus stiff yarns tend to move towards the yarn center to avoid being strained. As the specimens were pre-tensioned prior to testing, this eliminated the possibility that the effect is induced by yarn slack and inaccurate test length. In the second stage, the tensile stress-strain curve exhibits an increased slope. This can be explained by the fact that the two stiff yarns start to take more loads when they migrate to the yarn core and jam together; thereby, the tensile behavior of the 4-ply auxetic yarn is mainly dependent on that of stiff yarns at this stage.

Correlated Poisson's ratio versus tensile strain for the 4-ply auxetic yarn sample A-2 is shown in Figure 9b. It is observed that the negative Poisson's ratio effect first increased and then gradually decreased with increasing the tensile strain until the yarn was broken. Coupled with the tensile stress-strain curve, the increase in negative Poisson's ratio once again supported that the resulting graph well represents the actual extension of the 4-ply auxetic yarn; since taking up the slack of the yarn, if any, should result in a positive Poisson's ratio. Maximum negative Poisson's ratio behavior is obtained at a strain of around 0.033, where stage 2 just starts. This can be attributed to the migration effect of stiff yarns in the auxetic plied yarn structure. At a low tensile strain, the soft

yarns are pushed outward by the stiff yarns so that the transversal strain of the auxetic yarn increases rapidly. Under high axial extension, yarn core starts to jam with stiff yarns. In this case, although the transversal strain decreases due to the cross-sectional contraction of the constituent yarns, the plied yarn is still auxetic as its instantaneous width is still bigger than its starting width before breakage.

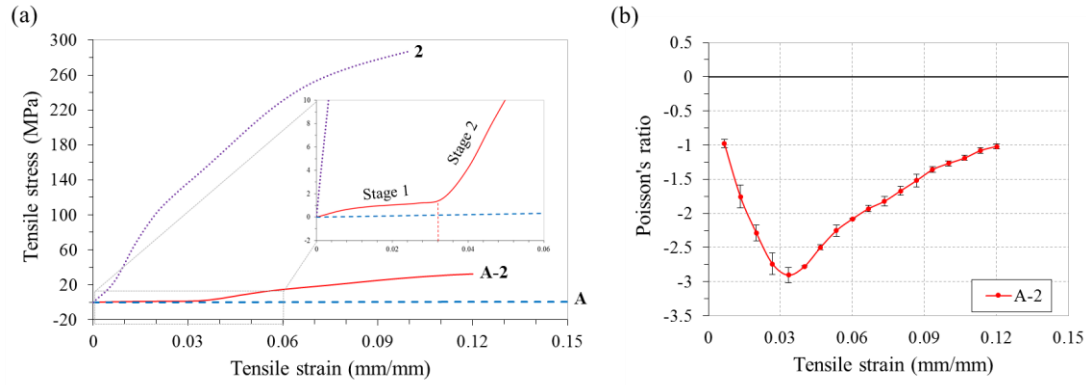

Figure 9 (a) Typical tensile stress-strain curves of 4-ply auxetic yarn sample A-2 and its constituent single yarns. The inset shows the enlargement at small stress; (b) Correlated Poisson's ratio-axial strain curve.

4.2 Effect of soft yarn diameter

To investigate the influence of the diameter of soft yarn on the tensile and deformation behavior of the 4-ply auxetic yarn structure, comparisons were conducted between different auxetic yarn samples made with the same stiff yarn but soft yarns of different diameters (2.18 mm and 1.14 mm respectively). Two groups of samples A-1/B-1 and A-2/B-2 were used for evaluation and the respective tensile stress-strain curves are depicted in Figures 10a and 10b, respectively. It can be seen that samples which have a finer soft yarn in their respective group demonstrate an earlier onset of stage 2 during

the tensile process, accompanying with a higher ultimate tensile strength. For sample B-1, the division of the two stages even becomes indistinguishable. The Poisson's ratio-tensile strain curves of these samples are shown in Figures 11a and 11b. It can be seen that the reduction in soft yarn diameter results in a sharp increase in negative Poisson's ratio at low strains, and the maximum negative Poisson's ratio is achieved earlier and the deviation begins to decrease with increasing the tensile strain.

It is believed that these differences occurred because relative position of the stiff yarns is dependent on the thickness of the soft yarns. Under the zero strain, the two stiff yarns are separated by the two soft yarns to form a 4-ply auxetic yarn structure. When a finer soft yarn is selected in a 4-ply auxetic yarn structure, the distance from the center of the stiff yarns to the center of the plied yarn becomes shorter. Accordingly, the stiff yarns can reach the yarn core shortly, thereby the migration of stiff yarn is expedited.

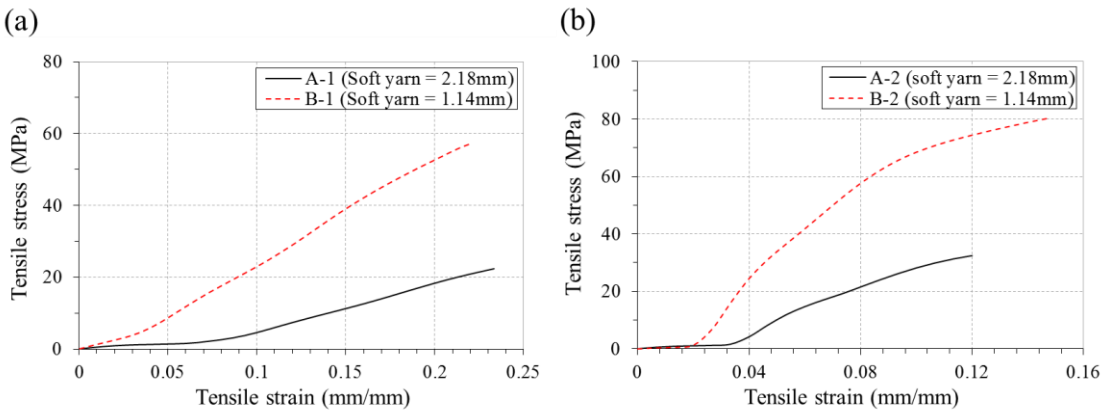

Figure 10 Tensile stress-strain curves: (a) sample A-1 and sample B-1; (b) sample A-2 and sample B-2.

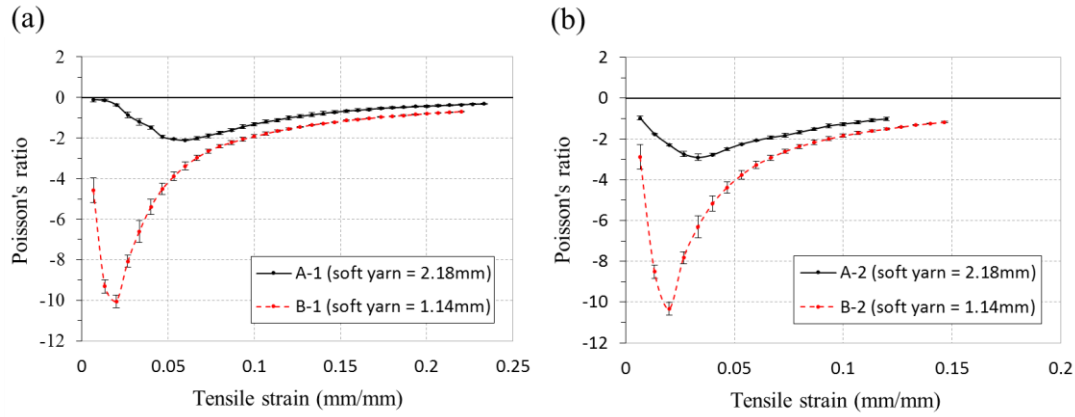

Figure 11 Poisson's ratio-tensile strain curves: (a) sample A-1 and sample B-1; (b) sample A-2 and sample B-2.

4.3 Effect of tensile modulus of stiff yarn

To investigate the influence of tensile modulus of stiff yarn on the tensile and deformation behavior of the 4-ply auxetic yarn structure, comparisons were carried out between different auxetic yarn samples made with the same soft yarn but stiff yarns of different moduli (630 MPa and 1307 MPa respectively). Two groups of samples A-1/A-2 and B-1/B-2 were used for evaluation and the respective tensile stress-strain curves are shown in Figures 12a and 12b. The results show that samples which have a higher tensile modulus of stiff yarn in their respective group demonstrate an earlier onset of stage 2 during the tensile process. In addition, they have a steeper slope in stage 2 than samples which have a lower tensile modulus of stiff yarn, resulting in a higher ultimate tensile strength and lower extensibility. The Poisson's ratio-tensile strain curves of these samples are shown in Figures 13a and 13b. In Figure 13a, sample A-2 which has a higher tensile modulus stiff yarn yielded a higher negative Poisson's

ratio at low strains. However, when the soft yarn is replaced by soft yarn B, no obvious differences can be found between the two samples as shown in Figure 13b.

It should be noted that mechanical and deformation properties of the 4-ply auxetic yarn may be influenced to some extent by the frictional behavior between the soft yarn and different stiff yarn as well. However, quantitative measurement of the magnitude of effects of friction is likely to be difficult. Definite evidence indicates that tensile modulus of stiff yarn affects the tensile properties of the 4-ply auxetic yarn structure, which may be attributed to their difference in migration intensity. When the 4-ply auxetic yarn is being stretched, components with a higher tensile modulus tend to induce an inward migration. If the difference in tensile modulus between the soft yarns and stiff yarns becomes larger, a greater hoop tension will be generated in the helices of the stiff yarns and a higher migration intensity will be resulted. In other words, when stiff yarn 1 and stiff yarn 2 were separately used to fabricate 4-ply auxetic yarns, it would be easier for yarn 2 to push the soft yarns to the outside, thereby stage 2 in tensile tests is expedited. However, the effect of tensile modulus of stiff yarn on the auxetic behavior of the 4-ply auxetic yarns has not shown a clear correlation with the variation in tensile properties between these samples. It is implicated that the diameter of soft yarn imposes a significant contribution to the auxetic behavior of the yarn, so that the effect of tensile modulus of stiff yarn to the auxetic performance of the 4-ply auxetic yarn structure becomes less significant.

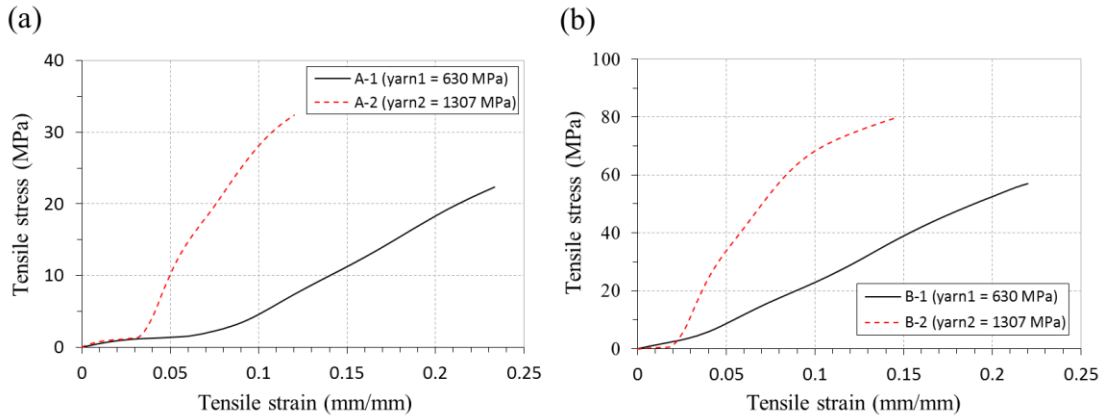

Figure 12 Tensile stress-strain curves: (a) sample A-1 and sample A-2; (b) sample B-1 and sample B-2.

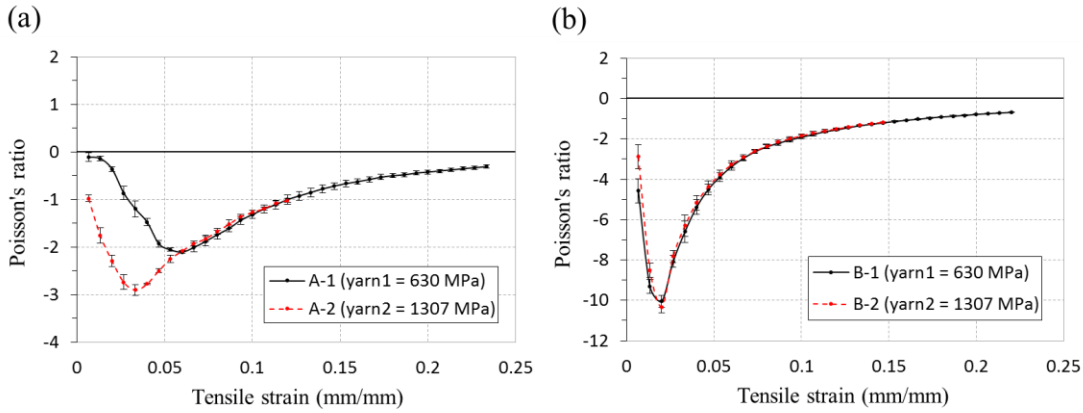

Figure 13 Poisson's ratio-tensile strain curves: (a) sample A-1 and sample A-2; (b) sample B-1 and sample B-2.

4.4 Effect of twist level

To investigate the influence of twist level on the tensile and deformation behavior of the 4-ply auxetic yarn structure, three twists levels (35, 51 and 65 turns/m) were employed to fabricate auxetic yarn samples (A-1-L, A-1 and A-1-H) and their respective tensile stress-strain curves are shown in Figure 14a. The results show that samples with different twist levels have a similar initial modulus; the initial stage of the curves are approximately the same but the length of this region varies. It is observed

that an increase in twist level retards the onset of stage 2, accompanying with an increase in extensibility. The Poisson's ratios-tensile strain curves of these samples are shown in Figure 14b. The results show that the degree of auxeticity is reduced with an increase in twist level at low strains. These phenomena can be explained by the fact that when the twist level is increased, the 4-ply auxetic yarn structure becomes more compact because of the binding effect of the twist. Therefore, the migration of stiff yarns is hindered and a poorer auxetic performance is resulted.

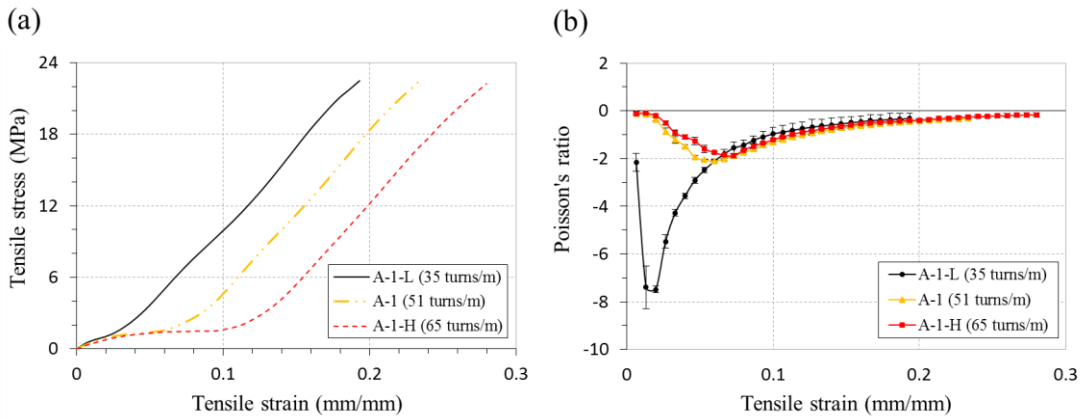

Figure 14 Comparisons among samples A-1-L, A-1 and A-1-H: (a) tensile stress-strain curves; (b) Poisson's ratio-tensile strain curves.

4.5 Cross-sectional deformation behavior

Sample A-1 was first selected as an example to study the cross-sectional deformation behavior of the 4-ply auxetic yarn structure. Its cross-sectional images at different strains from 0.00 to 0.15 are shown in Figures 15a to 15i respectively. Considering that the axes of the constituent yarns are not perpendicular to the axis of the resultant plied auxetic yarn structure, a minor distortion of the yarn cross-section is resulted. It is observed that the cross-section of the two stiff yarns in the 4-ply auxetic yarn remained

approximately circular while that of the soft yarns remained slightly elliptical. Under zero strain (Figure 15a), the two soft yarns were laid in the core region and separated the stiff yarns. At strain of 0.02 (Figure 15b), the stiff yarns started to migrate towards the yarn center to avoid being strained, while the soft yarns were moved away from the center accordingly. It can be attributed to the great difference in Young's modulus of the constituent yarns, as yarns with higher tensile modulus tend to exhibit an inward movement. Up to 0.11 strain (Figure 15g), the two stiff yarns completely migrated to the yarn core and jammed together. Since there was no room for any further movement, the two stiff yarns just closely packed together when tensile strain further increased to 0.15 (Figures 15i), and core-indentation phenomenon was observed. Although the degree of indentation increased with increasing strain, concerning that indentation occurred in the minor diameter direction only, the maximal thickness of the 4-ply auxetic yarn was unaffected by the indentation of the stiff yarns.

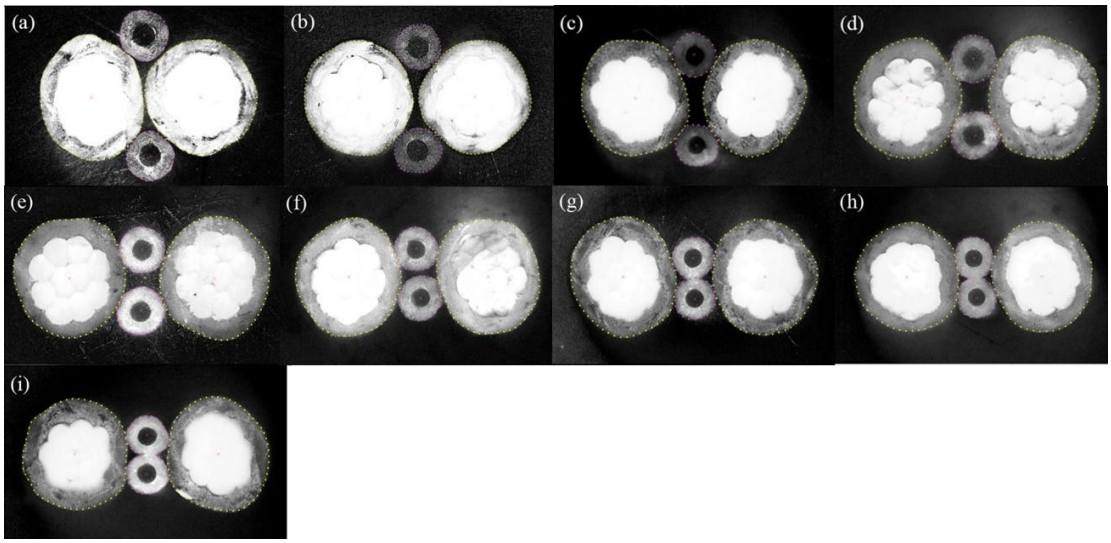

Figure 15 Cross-sectional images of sample A-1 at different strains: (a) 0; (b) 0.02; (c) 0.04; (d) 0.06; (e) 0.08; (f) 0.10; (g) 0.11; (h) 0.13; (i) 0.15.

Apart from sample A-1, cross-sectional samples of A-2 were also made to evaluate if there are any differences in their internal deformation behavior when the stiff yarn was different. The cross-sectional images of sample A-2 at different strains from 0.00 to 0.11 are shown in Figures 16a to 16g, respectively. A similar deformation trend can be observed, in which the two stiff yarns were initially separated by the two soft yarns laid in the core region and they appeared to migrate inwards when the 4-ply auxetic yarn was being stretched. Comparing the two different stiff yarns (yarn 1 and yarn 2) used in sample A-1 and A-2, the stiff yarns used in sample A-2 have a higher tendency to migrate inward. At strain of 0.08, free space could still be found for the stiff yarns to move further inwards in sample A-1 (Figure 15e); in contrast, the two stiff yarns in sample A-2 had already moved to the yarn center and contacted each other (Figure 16e). The results revealed that the migration intensity of stiff yarn is significantly affected by the tension variation of the constituent yarns, as discussed earlier. Besides, no indentation is observed after the two stiff yarns contacted with each other (Figures 16 e-g).

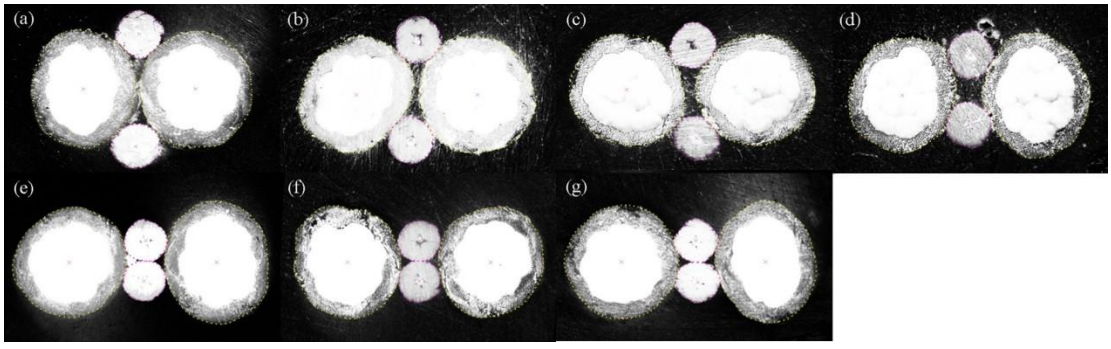

Figure 16 Cross-sectional images of sample A-2-Q at different strains: (a) 0.00; (b) 0.02; (c) 0.04; (d) 0.06; (e) 0.08; (f) 0.10; (g) 0.11.

Figures 17a and 17b present a comparative analysis of the Poisson's ratio of samples A-1 and A-2 obtained through the tensile test and cross-sectional measurements. It can be seen that the Poisson's ratio values obtained through the two methods are similar. Only a relatively larger deviation is observed in sample A-2 at high strains, which may be attributed to a minor slippage of the auxetic yarn when the specimens were embedded into the resin under high loads.

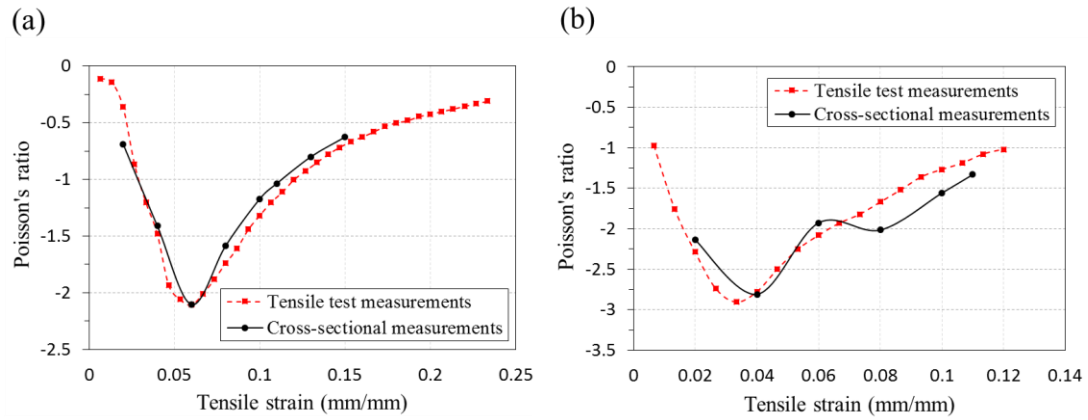

Figure 17 Poisson's ratios obtained with different methods: (a) sample A-1; (b) sample A-2.

4.6 Effect of helical structure

As explained before, three different auxetic yarn structures, i.e., DHY (sample A-1-D), 4-ply auxetic yarn (sample A-1) and 6-ply auxetic yarn (sample A-1-T) were fabricated to investigate the effect of helical structures on the deformation behavior of auxetic yarns. The Poisson's ratio-strain curves of these yarn structures are shown in Figure 18. It can be seen that DHY, 4-ply and 6-ply auxetic yarns have a significant variation in auxetic behavior under stretching. DHY A-1-D has the same kind of Poisson's ratio-strain curve and similar auxetic characteristics consistent with the references [23-25],

i.e., the Poisson's ratio is positive and increases with increasing tensile strain at the beginning of stretch, then decrease till its maximum negative value and finally increases toward zero until the yarn is broken. It is interesting to note that due to the core-wrap structure of the DHY, the initial elongation is inevitably accompanied with a positive Poisson's ratio. At the zero strain, the effective diameter of the DHY is determined by the helix radius of the stiff yarn. When the yarn is being stretched, the stiff yarn starts to straighten, thereby causing a decrease in its own helix radius. Since the initial increase in soft yarn helix radius is too small to alter the effective diameter of the auxetic yarn, a net decrease in effective diameter is resulted, which is correspondent to a positive Poisson's ratio.

Looking at the Poisson's ratio-tensile strain curve of the 4-ply auxetic yarn, sample A-1 exhibits a negative Poisson's ratio behavior throughout the entire tensile process. It is due to the fact that diameter of the auxetic yarn in a ply structure is determined by the helix radii of the soft yarns under zero tensile extension. Upon stretching, the migration of stiff yarns pushes the two soft yarns away from the center of the plied yarn, thereby causing an increase in soft yarns helix radii. As a result, the maximal diameter of the 4-ply auxetic yarn is increased with an achievement of negative Poisson's ratio.

For another auxetic plied yarn sample A-1-T made with 6 plies, Poisson's ratio value fluctuates but remains positive at low strains, accompanied by a high standard deviation. It may be attributed to the fact that the three stiff yarns rarely migrate to the yarn core at the same extent, so that diameter of the 6-ply auxetic yarn is unpredictable at low strains. Auxetic behavior is achieved lately at strain of 0.09, after a sudden sharp

increase in yarn diameter. A belated activation of auxetic behavior is resulted due to the fact that the auxetic plied yarn is more compact in a 6-ply structure so that the migration of stiff yarns is hindered.

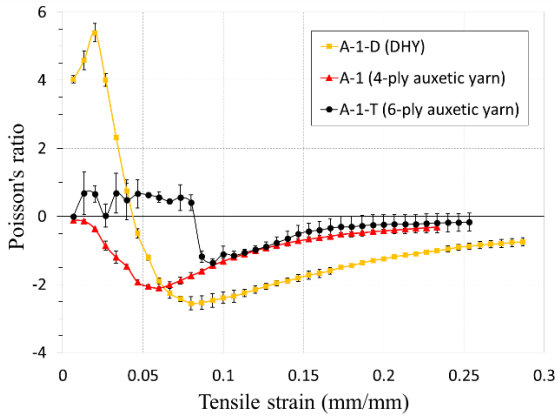

Figure 18 Poisson's ratio behavior of auxetic yarns made with different helical structures.

5. Conclusions and further research propositions

Tensile and deformation behavior of 4-ply auxetic yarns were experimental studied in this paper. A series of 4-ply auxetic yarns were fabricated and tested, the effects of various design parameters including diameter of soft yarn, tensile modulus of stiff yarn and twist level of the auxetic yarn were analyzed. On the other hand, the cross-sectional observations and measurements of 4-ply auxetic yarns under various extension levels were also conducted to study their cross-sectional deformation behavior. Finally, effect on the auxetic behavior arising from different helical structures was investigated. The main conclusions to be drawn from this study are:

(1) Negative Poisson's ratio of 4-ply auxetic yarn structure is more significant with a smaller soft yarn diameter, a higher tensile modulus of stiff yarn and a lower twist level.

(2) Deformation mechanism of this type of auxetic yarn structure has been verified through microscopic examination, that is, the migration of stiff yarns during extension pushes the soft yarns outward and induces an increase in maximal diameter of the auxetic yarn structure.

(3) The Poisson's ratios obtained by both the tensile tests and cross-sectional measurements have no evident differences.

(4) The helical structure has a significant effect on the auxetic behavior of auxetic yarns. Among the three HAY samples, 4-ply auxetic yarn is the only one exhibiting a negative Poisson's ratio behavior throughout the entire tensile process, indicating that auxetic plied yarns with a 4-ply structure are favorable for applications which require an auxetic performance at low strains or a fast response to produce auxetic effect upon stretching.

(5) The results indicate that there are certain possibilities of continuing the research work. One of them is to develop a finite element model to predict the negative Poisson's ratio behavior of the 4-ply auxetic yarns. Considering that friction between the constituent yarns may influence the mechanical and deformation properties of the 4-ply auxetic yarn, a clearer understanding on the effects is necessary. However, as mentioned above, quantitative measurement of the magnitude of effects of friction is likely to be difficult. It would be interesting to use an analytical model to investigate the frictional behavior along the contact

interfaces of the constituent yarns. In the model, contact friction can be simulated at various different values to evaluate the discrepancies between the simulated results and actual experimental data.

Acknowledgement

This work was supported by the Research Grants Council of Hong Kong Special Administrative Region Government in the form of a GRF project [grant number 515713].

References

[1] K.E. Evan, et al., Molecular network design. Nature 1991; 353(6340): 124.

[2] R. Lakes, Foam structures with a negative Poisson's ratio. Science 1987; 235(4792): 1038-1040.

[3] K.L. Alderson and K.E. Evans, The fabrication of microporous polyethylene having a negative Poisson's ratio. Polymer 1992; 33(20): 4435-4438.

[4] D. Mousanezhad, et al., Spiderweb honeycombs. International Journal of Solids and Structures 2015; 66: 218-227.

[5] E.A. Friis, R.S. Lakes, and J.B. Park, Negative Poisson's ratio polymeric and metallic foams. Journal of Materials Science 1988; 23(12): 4406-4414.

[6] L. Jiang, B. Gu, and H. Hu, Auxetic composite made with multilayer orthogonal structural reinforcement. Composite Structures 2016; 135: 23-29.

[7] N. Pour, et al., Auxetics at the molecular level: a negative Poisson's ratio in molecular rods. Angewandte Chemie International Edition 2006; 45(36): 5981-5983.

[8] K.E. Evans and K.L. Alderson, Auxetic materials: the positive side of being negative. Engineering Science and Education Journal 2000; 9(4): 148-154.

[9] T.C. Lim, Auxetic materials and structures. Singapore: Springer, 2015.

[10] Y. Liu, H. Hu, A review on auxetic structures and polymeric materials. Scientific Research and Essays 2010; 5 (10): 1052-1063.

[11] H. Hu, Z. Wang, and S. Liu, Development of auxetic fabrics using flat knitting technology. Textile Research Journal 2011; 81(14): 1493-1502.

[12] K. Alderson, et al., Auxetic warp knit textile structures. Physica Status Solidi B 2012; 249(7): 1322-1329.

[13] Y. Liu, et al., Negative Poisson's ratio weft-knitted fabrics. Textile Research Journal 2010; 856-863.

[14] Z. Wang and H. Hu, 3D auxetic warp-knitted spacer fabrics. Physica Status Solidi B 2014; 251(2): 281.

[15] Z. Wang and H. Hu, Tensile and forming properties of auxetic warp-knitted spacer fabrics. Textile Research Journal 2016; 0(00): 1-13.

[16] M. Glazzard and P. Breedon, Weft-knitted auxetic textile design. Physica Status Solidi B 2014; 251(2): 267.

[17] N. Ravirala, et al., Negative Poisson's ratio polyester fibers. Textile Research Journal 2006; 76(7): 540.

[18] K.L. Alderson, et al., Auxetic polypropylene fibres: Part 1 - Manufacture and characterisation. Plastics, Rubber and Composites 2002; 31(8): 344-349.

[19] J.R. Wright, et al., On the design and characterisation of low-stiffness auxetic yarns and fabrics. Textile Research Journal 2012; 82(7): 645-654.

[20] T.C. Lim, Semi-auxetic yarns. Physica Status Solidi B 2014; 251(2): p. 273-280.

[21] M.R. Sloan, J.R. Wright, and K.E. Evans, The helical auxetic yarn – A novel structure for composites and textiles geometry, manufacture and mechanical properties. Mechanics of Materials 2011; 43(9): 476-486.

[22] P.B. Hook, Auxetic mechanisms, structures & materials. Ph.D. thesis, School of Engineering and Computer Science, University of Exeter 2003.

[23] J.R. Wright, M.R. Sloan, and K.E. Evans, Tensile properties of helical auxetic structures: A numerical study. Journal of Applied Physics 2010; 108: 044905.

[24] Z. Du, et al., Study on negative Poisson's ratio of auxetic yarn under tension: Part 1 – Theoretical analysis. Textile Research Journal 2015; 85(5): 487-498.

[25] Z. Du, et al., Study on negative Poisson's ratio of auxetic yarn under tension: Part 2 – Experimental verification. Textile Research Journal 2015; 85(7): 768-774.

[26] A. Sibal and A. Rawal, Design strategy for auxetic dual helix yarn systems. Materials Letters 2015; 161: 740-742.

[27] S. Bhattacharya, et al., The variation in Poisson's ratio caused by interactions between core and wrap in helical composite auxetic yarns. Composites Science and Technology 2014; 102: 87-93.

[28] M. Vysanskav and P. Vintrova, Auxetic woven fabrics - Pores' parameters observation. Journal of Donghua University 2013; 30(5): 416-420.

[29] W. Miller, et al., A negative Poisson's ratio carbon fibre composite using a negative Poisson's ratio yarn reinforcement. Composites Science and Technology 2012; 72(7): 761-766.

[30] A. Alderson, Smart solutions from auxetic materials. 2011; Available from: http://www.med- techinnovation.com/articles/articles/article/20.

[31] A. Alderson, et al., Modelling of the mechanical and mass transport properties of auxetic molecular sieves: an idealised organic (polymeric honeycomb) host–guest system. Molecular Simulation 2005; 31(13): 897-905.

[32] Safe at work. (Bomb blast curtains). Professional Engineering Magazine 2010; 23(10): 38.

[33] Z. Ge, H. Hu, and S. Liu, A novel plied yarn structure with negative Poisson's ratio. The Journal of The Textile Institute 2016; 107(5): 578-588.

[34] H. Hu, S. Liu, Negative Poisson ratio yarn structure and manufacturing method thereof. Patent number CN103361811 A; 2012.

APPENDIX

Average Poisson's Ratio for Each Sample Measured during Tensile Testing

Table I Data of Sample A-1

Tensile strain (mm/mm)	Average Poisson's ratio	Standard Deviation	Tensile strain (mm/mm)	Average Poisson's ratio	Standard Deviation
0	--	--	0.120	-1.002	0.096
0.007	-0.110	0.095	0.127	-0.925	0.094
0.013	-0.140	0.044	0.133	-0.851	0.091
0.020	-0.359	0.050	0.140	-0.778	0.085
0.027	-0.864	0.140	0.147	-0.717	0.070
0.033	-1.200	0.173	0.153	-0.666	0.065
0.040	-1.477	0.073	0.160	-0.624	0.062
0.047	-1.931	0.071	0.167	-0.581	0.051

0.053	-2.058	0.034	0.173	-0.531	0.055
0.060	-2.105	0.031	0.180	-0.500	0.045
0.067	-2.009	0.089	0.187	-0.480	0.038
0.073	-1.882	0.099	0.193	-0.444	0.039
0.080	-1.739	0.091	0.200	-0.424	0.043
0.087	-1.610	0.065	0.207	-0.399	0.036
0.093	-1.439	0.089	0.213	-0.378	0.034
0.100	-1.318	0.081	0.220	-0.353	0.035
0.107	-1.200	0.083	0.227	-0.332	0.033
0.113	-1.110	0.085	0.233	-0.309	0.040

Table II Data of Sample A-2

Tensile strain (mm/mm)	Average Poisson's ratio	Standard Deviation	Tensile strain (mm/mm)	Average Poisson's ratio	Standard Deviation
0	--	--	0.067	-1.931	0.049
0.007	-0.976	0.065	0.073	-1.822	0.073
0.013	-1.754	0.165	0.080	-1.670	0.067
0.020	-2.288	0.118	0.087	-1.520	0.090
0.027	-2.737	0.160	0.093	-1.359	0.042
0.033	-2.903	0.112	0.100	-1.268	0.039
0.040	-2.776	0.010	0.107	-1.189	0.037
0.047	-2.498	0.038	0.113	-1.079	0.042
0.053	-2.251	0.084	0.120	-1.019	0.040
0.060	-2.080	0.009			

Table III Data of Sample B-1

Tensile strain (mm/mm)	Average Poisson's ratio	Standard Deviation	Tensile strain (mm/mm)	Average Poisson's ratio	Standard Deviation
0	--	--	0.113	-1.649	0.052
0.007	-4.574	0.598	0.120	-1.557	0.053
0.013	-9.314	0.338	0.127	-1.448	0.026
0.020	-10.054	0.303	0.133	-1.349	0.025
0.027	-8.072	0.292	0.140	-1.278	0.020
0.033	-6.603	0.537	0.147	-1.209	0.019
0.040	-5.390	0.366	0.153	-1.136	0.033
0.047	-4.512	0.274	0.160	-1.077	0.022

0.053	-3.892	0.216	0.167	-1.027	0.022
0.060	-3.375	0.187	0.173	-0.964	0.026
0.067	-2.970	0.130	0.180	-0.915	0.021
0.073	-2.645	0.090	0.187	-0.876	0.029
0.080	-2.399	0.094	0.193	-0.838	0.028
0.087	-2.220	0.108	0.200	-0.788	0.024
0.093	-2.056	0.096	0.207	-0.753	0.020
0.100	-1.919	0.090	0.213	-0.722	0.026
0.107	-1.785	0.085	0.220	-0.689	0.021

Table IV Data of Sample B-2

Tensile strain (mm/mm)	Average Poisson's ratio	Standard Deviation	Tensile strain (mm/mm)	Average Poisson's ratio	Standard Deviation
0	--	--	0.080	-2.364	0.235
0.007	-2.874	0.614	0.087	-2.158	0.226
0.013	-8.515	0.919	0.093	-1.988	0.219
0.020	-10.330	0.666	0.100	-1.840	0.198
0.027	-7.823	0.499	0.107	-1.711	0.200
0.033	-6.305	0.343	0.113	-1.596	0.174
0.040	-5.165	0.382	0.120	-1.503	0.166
0.047	-4.372	0.327	0.127	-1.408	0.146
0.053	-3.758	0.328	0.133	-1.310	0.155
0.060	-3.272	0.303	0.140	-1.237	0.136
0.067	-2.922	0.249	0.147	-1.167	0.131
0.073	-2.607	0.236			

Table V Data of Sample A-1-L

Tensile strain (mm/mm)	Average Poisson's ratio	Standard Deviation	Tensile strain (mm/mm)	Average Poisson's ratio	Standard Deviation
0	--	--	0.100	-0.968	0.275
0.007	-2.166	0.382	0.107	-0.891	0.287
0.013	-7.394	0.903	0.113	-0.817	0.307
0.020	-7.483	0.149	0.120	-0.742	0.287
0.027	-5.480	0.277	0.127	-0.679	0.314
0.033	-4.275	0.135	0.133	-0.632	0.287

0.040	-3.562	0.112	0.140	-0.589	0.296
0.047	-2.910	0.123	0.147	-0.547	0.269
0.053	-2.477	0.102	0.153	-0.492	0.251
0.060	-2.111	0.079	0.160	-0.458	0.239
0.067	-1.806	0.190	0.167	-0.407	0.241
0.073	-1.555	0.239	0.173	-0.391	0.231
0.080	-1.437	0.223	0.180	-0.363	0.246
0.087	-1.229	0.174	0.187	-0.343	0.240
0.093	-1.086	0.233	0.193	-0.319	0.225

Table VI Data of Sample A-1-H

Tensile strain (mm/mm)	Average Poisson's ratio	Standard Deviation	Tensile strain (mm/mm)	Average Poisson's ratio	Standard Deviation
0	--	--	0.160	-0.540	0.064
0.007	-0.107	0.040	0.167	-0.500	0.069
0.013	-0.100	0.010	0.173	-0.480	0.037
0.020	-0.200	0.075	0.180	-0.460	0.040
0.027	-0.500	0.089	0.187	-0.434	0.046
0.033	-0.935	0.137	0.193	-0.410	0.052
0.040	-1.095	0.095	0.200	-0.387	0.058
0.047	-1.261	0.153	0.207	-0.361	0.054
0.053	-1.591	0.152	0.213	-0.326	0.071
0.060	-1.745	0.043	0.220	-0.308	0.076
0.067	-1.861	0.044	0.227	-0.285	0.069
0.073	-1.877	0.075	0.233	-0.252	0.064
0.080	-1.644	0.075	0.240	-0.237	0.069
0.087	-1.479	0.116	0.247	-0.223	0.073
0.093	-1.343	0.036	0.253	-0.211	0.077
0.100	-1.221	0.069	0.260	-0.198	0.081
0.107	-1.087	0.043	0.267	-0.187	0.085
0.113	-0.985	0.061	0.273	-0.176	0.089
0.120	-0.888	0.059	0.280	-0.165	0.092
0.127	-0.832	0.016	0.287	-0.152	0.090
0.133	-0.767	0.036	0.293	-0.138	0.086
0.140	-0.704	0.029	0.300	-0.125	0.082
0.147	-0.652	0.054	0.307	-0.112	0.078

0.153	-0.600	0.058

Table VII Data of Sample A-1-D

Tensile strain (mm/mm)	Average Poisson's ratio	Standard Deviation	Tensile strain (mm/mm)	Average Poisson's ratio	Standard Deviation
0	--	--	0.147	-1.808	0.094
0.007	4.027	0.110	0.153	-1.724	0.120
0.013	4.584	0.270	0.160	-1.666	0.124
0.020	5.397	0.266	0.167	-1.594	0.098
0.027	4.010	0.188	0.173	-1.499	0.046
0.033	2.313	0.042	0.180	-1.441	0.031
0.040	0.749	0.232	0.187	-1.363	0.027
0.047	-0.502	0.135	0.193	-1.291	0.022
0.053	-1.214	0.073	0.200	-1.244	0.036
0.060	-1.897	0.093	0.207	-1.179	0.031
0.067	-2.260	0.140	0.213	-1.139	0.044
0.073	-2.414	0.076	0.220	-1.093	0.055
0.080	-2.551	0.193	0.227	-1.046	0.050
0.087	-2.529	0.196	0.233	-1.004	0.061
0.093	-2.469	0.200	0.240	-0.958	0.096
0.100	-2.391	0.169	0.247	-0.902	0.084
0.107	-2.338	0.175	0.253	-0.876	0.094
0.113	-2.250	0.112	0.260	-0.841	0.103
0.120	-2.148	0.103	0.267	-0.817	0.112
0.127	-2.054	0.085	0.273	-0.795	0.120
0.133	-1.958	0.073	0.280	-0.765	0.116
0.140	-1.892	0.081	0.287	-0.744	0.121

Table VIII Data of Sample A-1-T

Tensile strain (mm/mm)	Average Poisson's ratio	Standard Deviation	Tensile strain (mm/mm)	Average Poisson's ratio	Standard Deviation
0	--	--	0.133	-0.769	0.174
0.007	0.000	0.000	0.140	-0.655	0.223
0.013	0.680	0.628	0.147	-0.512	0.248
0.020	0.661	0.236	0.153	-0.436	0.237

0.027	0.025	0.338	0.160	-0.400	0.250
0.033	0.683	0.580	0.167	-0.343	0.278
0.040	0.483	0.587	0.173	-0.306	0.300
0.047	0.666	0.415	0.180	-0.302	0.300
0.053	0.634	0.018	0.187	-0.269	0.302
0.060	0.564	0.154	0.193	-0.246	0.290
0.067	0.445	0.076	0.200	-0.237	0.280
0.073	0.556	0.378	0.207	-0.223	0.281
0.080	0.405	0.230	0.213	-0.229	0.274
0.087	-1.176	0.168	0.220	-0.222	0.266
0.093	-1.362	0.113	0.227	-0.204	0.278
0.100	-1.104	0.225	0.233	-0.192	0.279
0.107	-1.146	0.140	0.240	-0.181	0.264
0.113	-1.066	0.108	0.247	-0.176	0.257
0.120	-0.973	0.108	0.253	-0.166	0.259
0.127	-0.887	0.139			